

MINIATURIZATION IN X-RAY AND GAMMA-RAY SPECTROSCOPY

Jan s. Iwanczyk, Yuzhong J. Wang
Xsirius, Inc., 4640 Admiralty Way, Suite 214, Marina del Rey, CA 90292

James G. Bradley
Jet Propulsion Laboratory, 4800 Oak Grove Drive, Pasadena, CA 91109

Abstract:

The paper presents advances in two new sensor and miniaturized associated electronics technologies which, when combined, can allow for very significant miniaturization, and the reduction of weight and power consumption in x-ray and gamma-ray spectroscopy systems:

1. Mercuric iodide (HgI_2) x-ray technology, which allows for the first time the construction of truly portable, high-energy resolution, non-cryogenic x-ray fluorescence (XRF) elemental analyzer systems, with parameters approaching those of laboratory quality cryogenic instruments.
2. The silicon avalanche photodiode (APD), which is a solid-state light sensitive device with internal amplification, capable of uniquely replacing the vacuum photomultiplier tube in scintillation gamma-ray spectrometer applications, and offering substantial improvements in size, ruggedness, low power operation and energy resolution.
3. Miniaturized (hybridized) low noise, low power amplification and processing electronics, which take full advantage of the favorable properties of these new sensors and allow for the design and fabrication of advanced, highly miniaturized x-ray and gamma-ray spectroscopy systems.

The paper also presents experimental results and examples of spectrometric systems currently under construction. The difficulties for future developments are discussed.

Mercuric iodide (HgI_2) technology:

Mercuric iodide (HgI_2) occurs in two main phases, tetragonal alpha- HgI_2 and orthorhombic beta HgI_2 . The tetragonal alpha- HgI_2 is stable at room temperature and undergoes a reversible transition to the orthorhombic phase at about 130°C. Alpha- HgI_2 single crystals usually are grown either by physical vapor transport at temperatures in the range of 100-115°C [1], or in solution at 25°C by decomplexing of dimethylsulfoxide- HgI_2 complexes [2]. Crystals grown from the vapor are characterized by better charge transport properties [3]. Table I lists selected properties of HgI_2 crystals. The current, most widely used vapor-growth technique was introduced by Scholz [4], and subsequently modified by different laboratories [1,5]. Another method, also used, is the growth of HgI_2 platelet crystals by polymer-assisted vapor transport [6,7]. The latter method yields relatively small sized single crystals.

Prior to detector fabrication, the as-grown crystals are sawed into slices, polished, and then etched in an aqueous solution of KIF. Electrodes are deposited onto both sides of a slice of HgI_2 single crystal. For x-ray applications, usually Palladium of 100-200 Å thickness is used as the electrode material. A guard ring structure is employed in order to reduce surface leakage current and improve the electric field distribution in the active part of the detector. The unit is then mounted onto a ceramic substrate for mechanical support. The surface of the detector is passivated and protected from the environment by a very thin (1-3 µm) plastic encapsulant. The Union Carbide Parylene process has been adopted for this purpose. Detectors are produced in different shapes and sizes, ranging from a few mm² up to several cm². Techniques have been developed to fabricate either single or multiple detectors on the same crystal slice. In addition, more complex, multi-element detectors have been designed in the form of submodules that can be aggregated into large linear or two dimensional arrays. A typical detector leakage current is in the range of 0.08-0.5 pA/mm² at room temperature, depending on the specific crystal and applied bias voltage. High energy-resolution detectors are constructed to exhibit the lowest electronic noise and the

best possible charge collection. Their capacitances are kept below 1 pF. A reduction of the electronic noise level of a spectroscopy system, as well as an enhancement of the charge collection, can be achieved by cooling the detector and the input Field Effect Transistor (FET), and can be accomplished using miniature thermoelectric (Peltier) coolers. These small, single stage coolers are very compact (less than 0.3 cm³) and use very little power (250 mW) to achieve an effective temperature in the range -10 to 0°C. Properly fabricated detectors show very good long term stability and reliability of their performance under various ambient conditions, including high vacuum and temperature cycling [8]. Also, HgI₂ detectors exhibit excellent radiation damage resistance in comparison to other semiconductor detectors [9,10].

In summary, it has been found that HgI₂ possesses a number of properties that make it very attractive for room temperature x-ray detectors that are capable of high energy resolution.

TABLE I

Property	Value
Crystal Structure	Tetragonal (low T, red) Orthorhombic (high T, yellow)
Lattice Parameters	a = b = 4.361 Å, c = 12.450 Å
Density	6.4 g/cm ³
Melting Point	259°C
Phase Transition Temperature	177°C
Dielectric Constant	8.80 1.2i (at 5461 Å)
Index of Refraction	2.71 (at 5890 Å), 2.67 (at 6328 Å)
Band Gap	2.13 eV
Electrical Resistivity	~10 ¹³ ohm-cm
Electron Mobility	~ 100 cm ² /Vs at 300K
Hole Mobility	~ 4 cm ² /Vs at 300K
(μ) _e	< 10 ⁻³ cm ² /V
(μ) _h	< 10 ⁻⁵ cm ² /V
Energy per e-h pair	4.2 eV (measured)
Fano factor	0.1

Avalanche photodiode (APD) technology:

The most common "reach-through" APD structure was introduced by R.J. McIntire over two decades ago [11], and devices based upon it have been produced since then in many commercial companies. This structure allows one to achieve reliable and high performance devices with useful internal gain. These devices have found many applications, including those in short wavelength communications. However, due to their small active areas (limited to only a few square millimeters, at most), they never offer Cd any real competition to PMTs in a wide range of applications.

Recently, though, newer large area avalanche photodiodes have become available [12, 13]. These newer APDs are based upon a construction which utilizes a highly uniform, neutron-transmutation-doped silicon, thus allowing for the formation of a large area, uniform junction. Breakdown at the junction periphery is prevented, even with very high electric fields, by physically beveling the edges of the diode, and by specially treating the edge [13]. This technology now offers APDs with diameters much larger than 0.5 in., capable of operating at voltages in excess of 2 kV. APDs of 200 mm² area have typical surface dark currents of 200 nA, and bulk dark currents of less than 0.5 nA. The large area APDs can operate with gains up to 1,000. The parameter k_{eff}, which determines the noise performance at high gain [11], is approximately 0.0015, compared to 0.0025 quoted for the best "reach-through" structures. The typical quantum efficiency of current devices is ~85% in the 550-1000 nm range of photon

wavelengths, falling to a few percent at 300 nm, although there is an extensive effort being pursued to improve the sensitivity of APDs at short wavelengths to extend its response into the UV region. Such APDs offer an overall reduction in system size and complexity, compared with general purpose PMTs, as well as improved ruggedness, reliability and longevity. Additional advantages include a linear response over a 7 decade range of signal intensities. The new photodetector draws less power than an equivalent PMT, and operates from a single high voltage. Since it is immune to the effects of magnetic fields it requires no shielding.

Miniaturized Amplification and Processing Electronics:

The development of miniaturized, low noise, low power amplification and processing electronics allows one to take full advantage of the new sensors and to develop highly compact spectroscopy systems. HgI₂ systems benefit much more strongly by the use of hybridized electronics than do the bulky Si[Li] or Ge cryogenically cooled systems, which require liquid nitrogen and high vacuum operation. We have concentrated our efforts towards the development of high performance electronics for space applications and synchrotron radiation applications.

a) Preamplifiers

A pulsed-light feedback preamplifier has been constructed using hybrid techniques in a standard 24-pin, dual-in-line package (DIP). The preamplifier has been tested with HgI₂ x-ray detectors, and the electronic noise level of the system was measured at below 20 electrons rms [14] at 12 μs shaping time, power consumption was 770 mW. Recently, a new design was implemented which allows for the further reduction of power consumption down to about 85 mW, without any deterioration in noise characteristics. The circuit is prepared for hybridization in a 14 pin dual-in-line package (0.79" x 0.47") and will weigh about 4 grams.

b) Amplifiers

A triangular shaping amplifier, including a wrap-around baseline restorer, computer controlled fine and coarse gains, and computer selectable shaping times, has been developed and hybridized in a 50-pin DIP package (1.5" x 2.6"). The total power consumption of the amplifier is about 2.6 W. The amplifier can work in conjunction with a recently developed pile-up rejector (PUR), which has also been hybridized in a separate 2.1" x 0.9" package. These circuits were tested with HgI₂ detectors for count rates of up to 175 kcps, and showed no practical differences with full sized commercial spectroscopy amplifiers at the selected shaping times. The details of the design and testing procedures are given elsewhere [15].

For space applications, the amplification circuit can often be simplified by using only single settings for the gain and shaping time. Also, pile-up rejection electronics can be eliminated for low count rate experiments. Our Dile suit effort in collaboration with the University of Chicago, for example, is concentrated on such a design, which besides the amplification and shaping circuitry involves a baseline restorer, a peak detector and a sample-and-hold circuit. The power consumption of this design is about 150 mW, and it can be hybridized in a 16 pin DIP (0.89" x 0.47") package.

c) Processing electronics

A quad single channel analyzer (q-SCA) that has four independent SCAs, each followed by 24 bit scalers, has been developed and hybridized in a 1.5" x 3.0" package. The circuit is built to be interfaced with a computer that can be used to set the threshold levels of the SCAs, and provide for the readout of scaler contents. Total power dissipation is only 0.8 W. A more detailed description of the design is given elsewhere [15].

For many applications, a miniaturized low power multichannel analyzer is much more desirable than a series of SCAs. There is an active effort involving the University of Chicago and the Max Planck Institute to construct such processing electronics, including the ADC and assorted memories, digital signal processors and interfaces. By using a low power, successive-approximation 12 bit ADC (Analog Devices AD7878), and by combining 3 channels (thus effectively reducing it to a 9 bit system), and

finally by incorporating Gatti corrections [16], it was possible to obtain differential nonlinearities below 1%.

Experimental Results:

Figure 1 shows a characteristic x-ray spectrum for copper taken with a HgI₂ spectrometer operating as an integral part of the Scanning Electron Microscope and Particle Analyzer (SEMPA) prototype instrument. The characteristic x-rays were excited by electrons. The spectrum shows well separated Cu K_α and Cu K_β lines at 8.0 and 8.9 keV, with an energy resolution of 218 eV (FWHM) (at the 8.0 keV peak). Also shown are Cu L lines (L_α, L_β at 928, 948 eV, respectively) exhibiting 190 eV (FWHM) energy resolution. Figure 2 presents a Ni target fluorescence spectrum measured with the same instrument used to obtain the data in Figure 1. In addition to the Ni K_α and K_β lines at 7.5 and 8.3 keV, the combined Ni L lines are clearly visible at 849 eV with an energy resolution of 182 eV (FWHM). The SEMPA instrument had been developed for NASA's Mariner Mark II Comet-Neutrons/Asteroids Flyby Mission to analyze cometary dust, and was designed to provide the simultaneous information of both an SEM image and the elemental composition of dust grain specimens.

Figure 3 shows an x-ray spectrum of meteorite Murchison, taken with a HgI₂ spectrometer inserted into the Alpha Backscattering Instrument. A ²⁴⁴Cm alpha source was used to excite fluorescent x-rays from the sample. The Alpha-X Backscattering Instrument is under development in collaboration with the University of Chicago and the Max Planck Institute to analyze the composition of the Martian surface on the upcoming Mars 94 Mission.

Figure 4 presents a composite of x-ray spectra from different targets taken with a HgI₂ array. For relatively low count rate conditions (10 kcps) the following FWHM energy resolutions were obtained: 252 eV at 5.9 keV (Mn-K_α), 380 eV at 17.44 keV (Mo-K_α), and 479 eV at 24.14 keV (In-K_α). The spectra shown here were measured using the Stanford Synchrotron Radiation Laboratory's (SSRL) intense SR beams to excite elemental targets. HgI₂ detector arrays are being developed to enhance the benefits of synchrotron radiation sources in several fields of biological and materials science research. Recently, a two dimensional array of twenty elements has been fabricated, and construction of a 100 element detector array system has also begun.

Figures 5-9 report results obtained with a large area Avalanche Photodiode (APD). An avalanche photodiode was optically coupled to a CsI(Tl) scintillator (1.27 mm X 1.27 mm). The diameter of the APD was 15 mm. The APD/scintillator detector was tested by using different radiation sources. Figure 5 shows the gamma ray spectrum taken using a ¹³⁷Cs source. An energy resolution of 6.24% for the ¹³⁷Cs (662 keV) gamma line was obtained. Figure 6 shows an energy resolution of 7.7% for a 511 keV line (²²Na source) and Figure 7 shows an energy resolution of 23.1% for an 80 keV line (¹³³Ba source). The APD/scintillator combination was also tested with a 122 keV line (⁵⁷Co source) and the energy resolution was 16.3% (cf. figure 8). Another APD was also measured with a BGO scintillator irradiated with a ²²Na source (511 keV and 1275 keV gamma rays). Figure 9 shows the spectrum taken at 0°C. The FWHM at 511 keV is 11.2%. The same BGO crystal was measured with a PM tube, and the FWHM at 511 keV was 11.6%. In Figure 9, the bismuth escape peak (511 keV - 76 keV) was well distinguished on the left shoulder of 511 keV peak, a feature which is not possible to observe with a PM tube.

Future Development:

The requirements for space instrumentation are in many aspects very similar to that for terrestrial field applications. The reduced weight, power and size of the spectrometer can lead to extremely attractive portable x-ray fluorescence instruments and gamma-ray spectrometers for environmental pollution monitoring, geological exploration, marine mineral analysis, archeometry, and industrial material quality assurance. One can foresee new generation, energy dispersive, detector array gamma cameras which are able to efficiently reject Compton scatter, and thereby enhance medical or industrial images.

Our continuing effort is directed toward the improvement in HgI₂ crystal growth methods, the refinement of detector fabrication techniques, and to the development of new designs of the associated electronics. In the area of APDs, we are putting an extensive effort into developing large scale, two dimensional detector arrays. The development of miniaturized, low noise, low power processing electronics allows one to take full advantage of the favorable properties of these new sensors. Rapid progress in commercial operational amplifiers, CMOS microcomputers and other hardware logic elements with lower power consumption, reduced noise, and lower cost, strongly benefits the portable x-ray spectrometric instrumentation field. For large scale detector arrays, these advances can be translated into a possibility for constructing very powerful systems with affordable costs per electronics channel.

Acknowledgments:

The research work described in this paper was supported by the National Aeronautics and Space Administration, Contracts NASW-4432 and NAS5-33045; NIH Grant No. 5R01 GM37161. In addition the authors wish to acknowledge the support and helpful assistance of Mr. Bart Dancy in the construction of the HgI₂ spectrometer probes, Ms. Fanny Riquelme for the fabrication of the HgI₂ detectors, Mr. Marek Szawlowski of Advanced Photonix, Inc. for the results of his measurements on APDs, and Mr. Wayne Schnepfle for assistance in preparation of this paper.

References:

- [1] M. Schieber, W.E. Schnepfle and L. VandenBerg, "Vapor Growth of HgI₂ by periodic Source or Crystal Temperature Oscillation", J. Crystal Growth 33 (1976) 125.
- [2] Y.F. Nicolau, M. Dupuy and Z. Kabsch, "Differential Scanning Calorimetry and Scanning Cathodoluminescence Microscopy Study of Doped (Ga) I₂ Crystals", Nucl. Instr. and Meth. A283 (1989) 149-166.
- [3] A.J. Dabrowski, "Solid-State Room-Temperature Energy-Dispersive X-Ray Detectors", Adv. X-ray Anal. 25 (1982) 1.
- [4] I.L. Scholtz, "On Crystallization by Temperature-Gradient Reversal", Acta Electronica 17 (1974) 69.
- [5] H.A. Landronds, "Review of Mercuric Iodide Development Program in Santa Barbara", Nucl. Instr. and Meth. 213 (1983) 5-12.
- [6] S.L. Faile, A.J. Dabrowski, G.C. Huth, and J.S. Iwanczyk, "Mercuric iodide (HgI₂) Platelets for X-Ray Spectroscopy Produced by Polymer Controlled Growth", J. Crystal Growth 50 (1980) 17-52.
- [7] J.B. Barton, A.J. Dabrowski, J.S. Iwanczyk, J. H. Kusmiss, G. Ricker, J. Vallerger, A. Warren, M.R. Squillante, S. Misra and G. Entine, "Performance of Room-Temperature X-ray Detectors Made from Mercuric Iodide (HgI₂) Platelets" Advances in X-ray Analysis Vol. 25, Plenum Press, NY, (1981) 31-37.
- [8] J.S. Iwanczyk, Y.J. Wang, J.G. Bradley, J.M. Conley, A.L. Albee and T.E. Economou, "Performance and Durability of HgI₂ X-Ray Detectors for Space Missions", IEEE Trans. Nucl. Sci. 36, No. 1 (1989) 841-845.
- [9] T.E. Economou, J.S. Iwanczyk and A. Turkevich, "The X-Ray Mode of the Alpha Particle Analytical Instrument", Proceeding of the Lunar and Planetary Sci. XXII Conf., (1990) 309-310.
- [10] B.E. Patt, R.C. Dolin, T. M. Devore, J.M. Markakis, J.S. Iwanczyk, N. Dorri and J. Trombka, "Radiation Damage Resistance in Mercuric Iodide X-Ray Detectors", Nucl. Instr. and Meth. A299 (1990) 176-181.

- [11] P.P. Webb, R.J. McIntyre and J. Conradi, "Properties of Avalanche Photodiodes", RCA Review, June 1974, 234-278.
- [12] N. Gelazunas, et al., "Uniform Large-Area High-Gain Silicon Avalanche Radiation Detectors from Transmutation Doped **Silicon**" Applied Physics Letters, Vol. 30, No. 2, (1977)
- [13] J. Iwanczyk, "Light Responsive Avalanche Diode", U.S. Patent 5,057,892 (1991)
- [14] J.S. Iwanczyk, A.J. Dabrowski, B.W. Dancy, B.E. Patt, T.M. Devore, A. Del Duca, C. Ortale, W.F. Schnepple, J.E. Barksdale and T. J. Thompson, "An Ultra Low Noise, Low Power Hybrid Preamplifier for X-ray Spectrometry", IEEE Trans. Nucl. Sci. NS-34 (1987) 124-126.
- [15] J.S. Iwanczyk, N. Dorri, M. Wang, R.W. Szczepiot, A.J. Dabrowski, B. Hedman, K.O. Hodgson, and B.E. Patt, "20 Element HgI₂ Energy Dispersive X-ray Array Detector System", Presented at 1991 Nucl. Sci. Symp. Santa Fe, NM (Nov. 5-8, 1991) to be published in IEEE Trans. Nucl. Sci. 1992.
- [16] C. Cottini, E. Gatti, V. Svelto, "A New Method for Analog-to-digital Conversion", Nucl. Instr. and Meth. 24 (1963) 241.

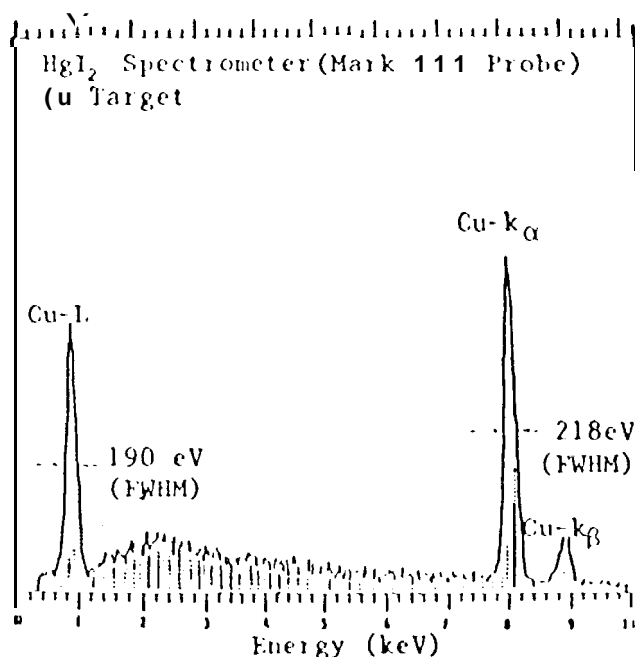


Figure 1. X-ray fluorescence spectrum for copper.

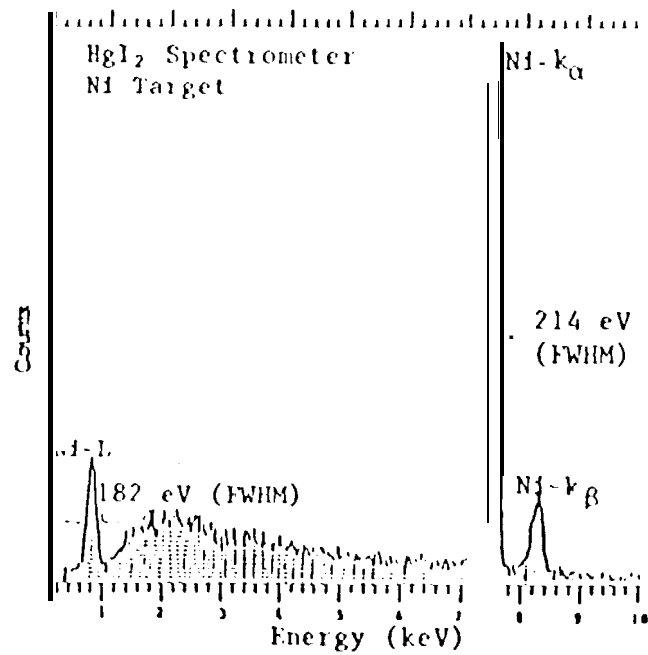


Figure 2. X-ray fluorescence spectrum for nickel.

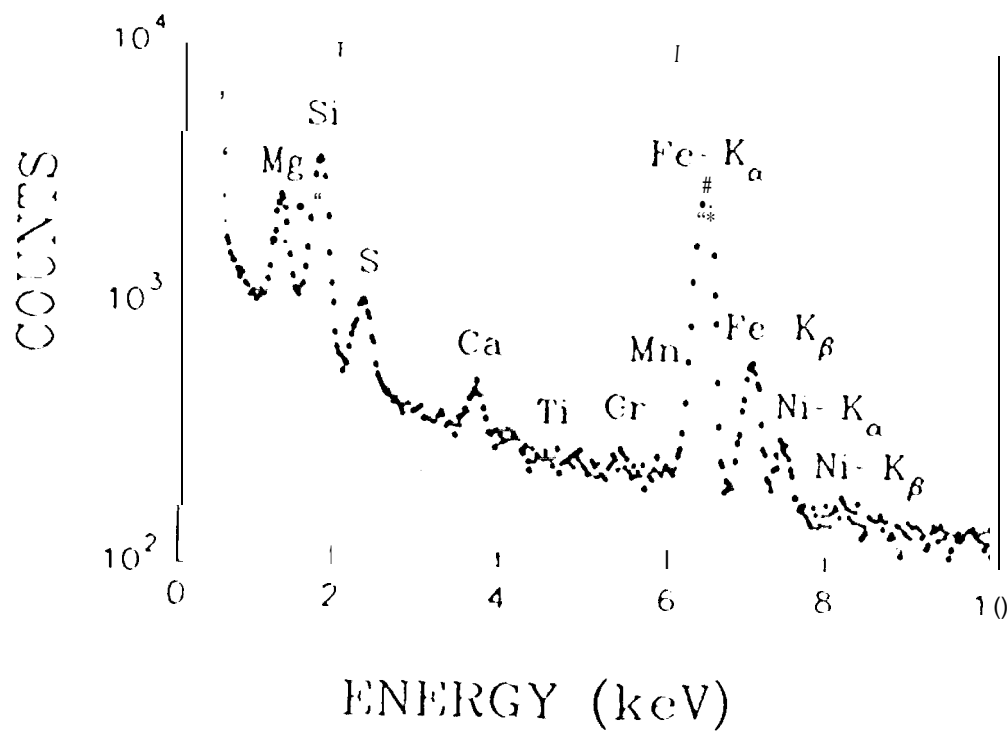


Figure 3. X-ray spectrum from a sample of meteorite Murchison taken with a HgI₂ detector probe (excited by a ²⁴⁴Cm source).

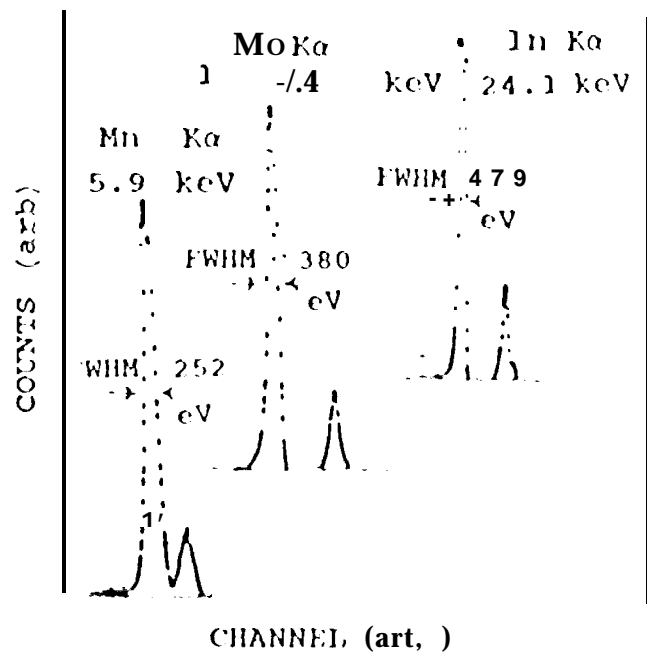


Figure 4. Spectra taken with HgI₂ array for: (a) Mn K; (b) Mo K; and (c) In K fluorescent emission lines.

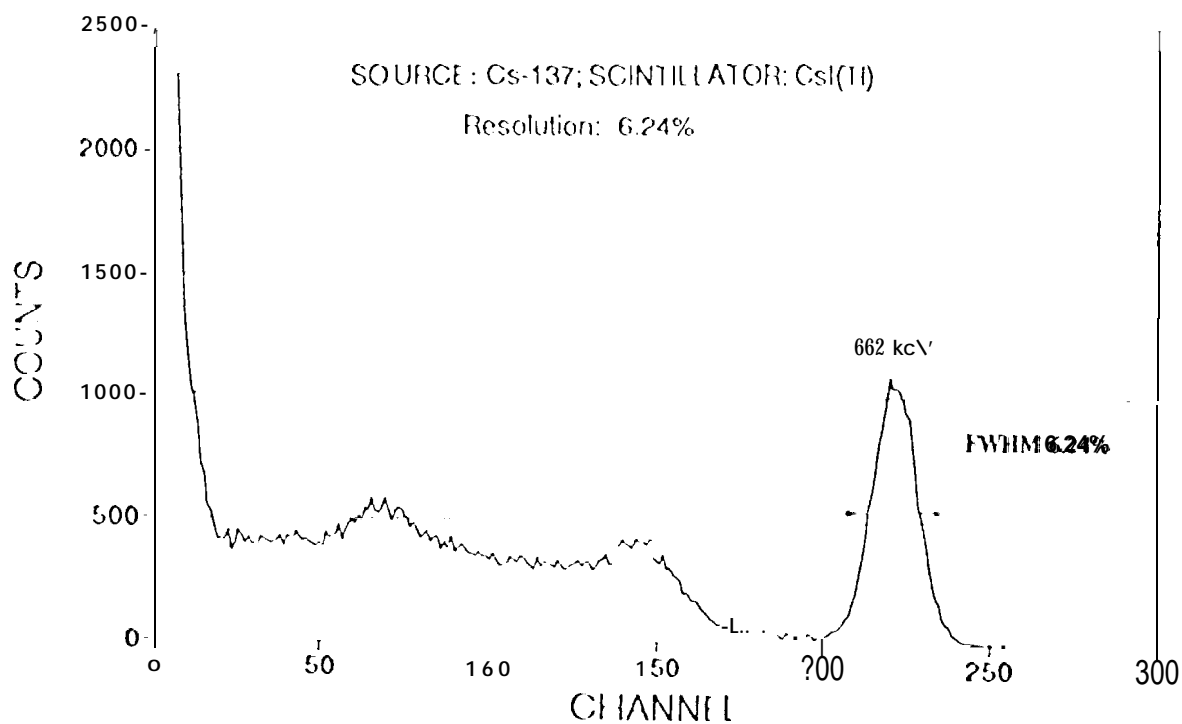


Figure 5. Spectrum from a ¹³⁷Cs source measured with an APD/CsI(Tl) detector.

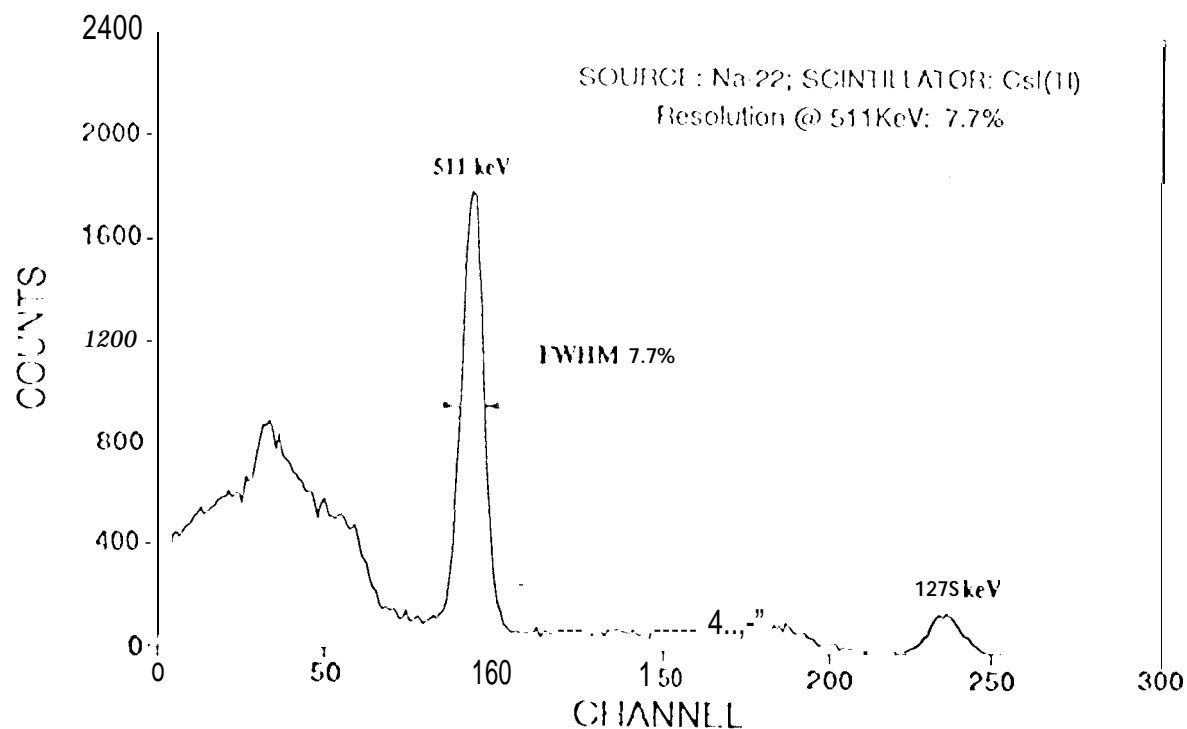


Figure 6. Spectrum from a ^{22}Na source measured with an APD/CsI(Tl) detector.

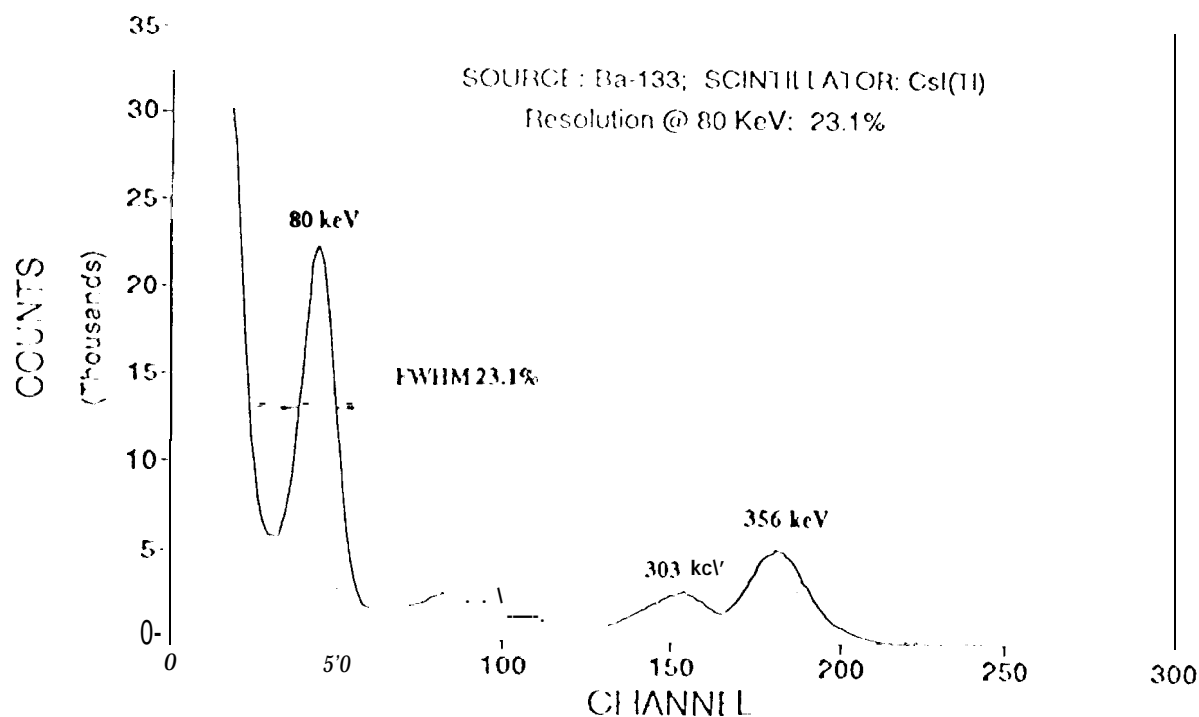


Figure 7. Spectrum from a ^{133}Ba source measured with an APD/CsI(Tl) detector.

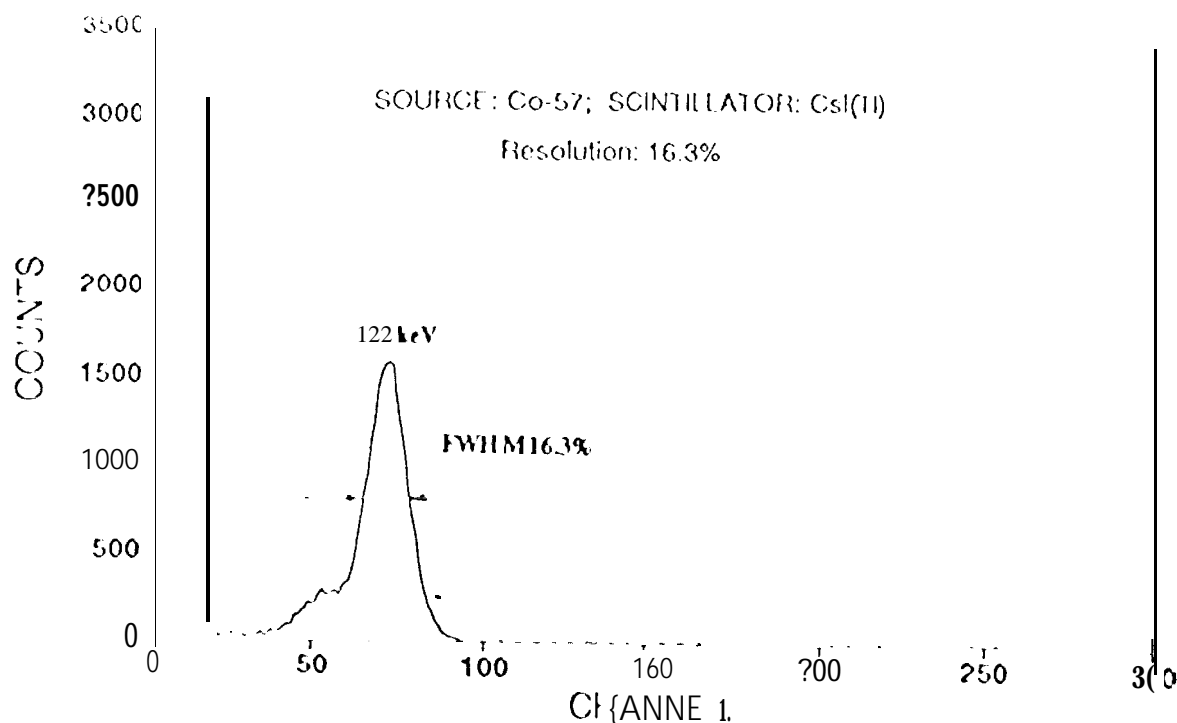


Figure 8. Spectrum from a ^{57}Co source measured with an APD/CsI (Tl) detector.

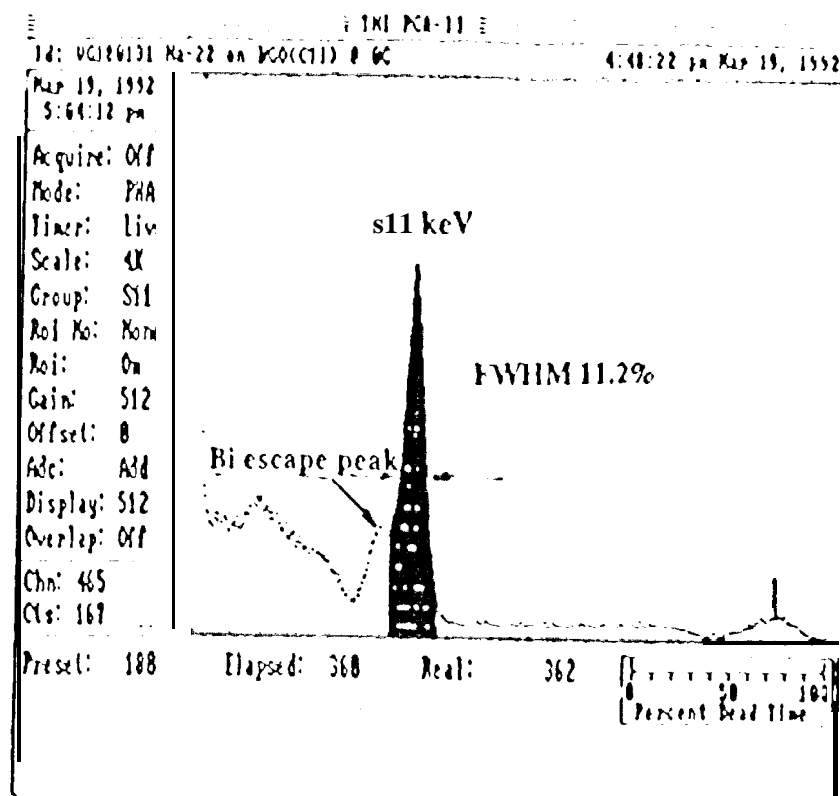


Figure 9. Spectrum from a ^{22}Na source measured with an APD/BGO detector.